

This is the peer reviewed version of the following article: *Bueno-López, J.I., Díaz-Hinojosa, A., Rangel-Mendez, J.R., Alatraste-Mondragón, F., Pérez-Rodríguez, F., Hernández-Montoya, V. and Cervantes, F.J. (2020), Methane production enhanced by reduced graphene oxide in an anaerobic consortium supplied with particulate and soluble substrates. J Chem Technol Biotechnol, 95: 2983-2990*, which has been published in final form at: <https://doi.org/10.1002/jctb.6459>

This article may be used for non-commercial purposes in accordance with Wiley Terms and Conditions for Use of Self-Archived Versions.

Methane production enhanced by reduced graphene oxide in an anaerobic consortium supplied with particulate and soluble substrates

Short title: Enhanced methanogenesis with reduced graphene oxide

J. Iván Bueno-López^a, Alejandra Díaz-Hinojosa^b, J. Rene Rangel-Mendez^{a,*}, Felipe Alatríste-Mondragón^a, Fátima Pérez-Rodríguez^c, Virginia Hernández-Montoya^d and Francisco J. Cervantes^{e,*}

^aDivisión de Ciencias Ambientales, Instituto Potosino de Investigación Científica y Tecnológica (IPICYT), Camino a la Presa San José 2055, Col. Lomas 4a. Sección, 78216 San Luis Potosí, SLP, Mexico

^bFacultad de Ciencias Químicas, Universidad Autónoma de San Luis Potosí, Av. Manual Nava 6, San Luis Potosí, 78210 Mexico

^cCONACYT- Instituto Potosino de Investigación Científica y Tecnológica (IPICYT), Camino a la Presa San José 2055, Col. Lomas 4a. Sección, 78216 San Luis Potosí, SLP, Mexico

^dInstituto Tecnológico de Aguascalientes, Av. Adolfo López Mateos No. 1801 Ote., 20256, Aguascalientes, Ags., Mexico

^eLaboratory for Research on Advanced Processes for Water Treatment, Engineering Institute, Campus Juriquilla, Universidad Nacional Autónoma de México (UNAM), Blvd. Juriquilla 3001, 76230 Querétaro, Mexico

*Corresponding authors: E-mail address: rene@ipicyt.edu.mx (J.R. Rangel-Mendez) and FCervantesC@iingen.unam.mx (F.J. Cervantes)

ORCID numbers:

This article has been accepted for publication and undergone full peer review but has not been through the copyediting, typesetting, pagination and proofreading process which may lead to differences between this version and the Version of Record. Please cite this article as doi: 10.1002/jctb.6459

J. René Rangel-Mendez: 0000-0002-9499-205X

Francisco J. Cervantes: 0000-0002-8382-1757

Virginia Hernández-Montoya: 0000-0003-3545-497X

ABSTRACT

BACKGROUND: Graphene materials have extensively been applied in several industries due to their enhanced properties. Predictably, these materials also end up in wastewaters generated from industrial sectors, and their effects on biological treatment systems are poorly understood. The aim of the present study was to assess the acute effects of graphene oxide (GO) with three different degrees of reduction (reduced GO (rGO) produced with a reduction time of 1, 2 and 4 hours) on the methane production of an anaerobic consortium.

RESULTS: Synthesized rGO materials had a stimulatory effect increasing the maximum methanogenic activity (MMA) up to 14% and 114% when glucose and starch were provided as substrates, respectively, as compared to the MMA achieved in controls incubated in the absence of rGO. Reduction of GO promoted physical-chemical changes in its structure, such as removal of epoxy groups, which prevented grapping of starch granules by the produced rGO sheets and triggered a better interaction between the latter and microorganisms. Furthermore, this work showed that rGO stimulated starch disintegration into its components, thus accelerating its hydrolysis, which was ultimately reflected in a higher MMA when this particulate polymer was used as substrate.

CONCLUSION: This study reports for the first time the acute effects of rGO on the methanogenic activity of an anaerobic consortium supplied with both soluble and particulate substrates. This information is relevant to elucidate the effects of this graphene material in anaerobic microorganisms and to improve the performance of anaerobic systems during the treatment of industrial wastewaters.

Keywords: reduced graphene oxide; starch; anaerobic digestion; hydrolysis

Introduction

Graphene oxide (GO) is one of the main raw materials used in the manufacture of graphene-like products because it is easy to reduce by different physical methods, such as thermal treatment and laser irradiation, as well as electrochemical^{1, 2} and green chemical processes using vitamins, sugars, amino acids and natural extracts.³⁻⁶ Reduced graphene oxide (rGO), so called because not all oxygenated groups are removed in the reduction process, is expected to prevail in natural environments and in wastewater treatment plants, since GO can be reduced to rGO by bacterial respiration.^{7, 8} Therefore, the degree of reduction in rGO could vary depending on the conditions of the manufacturing process and the environmental conditions prevailing.

Several carbonaceous materials have been used to improve the biotransformation of a wide variety of pollutants as well as the methanogenic activity of anaerobic consortia. One of those materials is activated carbon, which showed an enhancement on methane yield, especially when it was supplied as a fine powder. Activated carbon increases methane production due to the porosity of its particles, which serve as a proper niche to support microbial growth. More recently, activated carbon derived from organic wastes has been shown to effectively enhance the reduction of N_2O by denitrifying microorganisms, in addition to improving methane production in anaerobic consortia.⁹ Additionally, the conductivity of activated carbon favors direct interspecies electron transfer (DIET).¹⁰ Carbon nanofibers have also been reported to enhance the anaerobic biotransformation of nitroaromatic compounds; moreover, chemical surface modification played a relevant role, indicating that functional groups, which are able to accept and donate electrons, such as quinone groups, take part as redox mediators.¹¹ In the field of carbon nanomaterials, GO was also applied as electron shuttle for the reduction of recalcitrant pollutants by methanogenic sludge, but the concentration used was 5 mg/L due to toxic effects found at higher concentrations.¹² In opposition to the toxic effect of GO, the use of carbon nanotubes, in concentrations in the range of grams, showed an increase in methane production in a dose-dependent manner, but these experiments suggested that DIET is not the driving factor for methane improvement and probably other factors, such as the adsorption capacity may contribute to these results.¹³

Application of graphene in anaerobic digestion processes, at concentrations between 30 and 120 mg/L, showed a stimulation effect on methane production, specially favoring acetoclastic methanogenesis. These studies include a comparison with quinones and revealed that these moieties failed to replicate graphene stimulation, concluding that graphene did not function as electron shuttle in this kind of systems and support DIET as the mechanism for the observed methane enhancement.¹⁴ rGO has also been reported to increase degradation processes, which was attributed to the electron shuttling capacity of its remaining oxygenated functional groups as evidenced by chemical and biological experiments using rGO with different reduction degree. Moreover, the results pointed out that the higher the reduction degree of rGO, the higher the reduction rate observed in the studied pollutants and suggested that the enrichment of carbonyl groups in rGO might be responsible for the enhanced degradation observed.^{15, 16} In all the previously discussed cases, the contaminants, as well as the substrates, were soluble. Therefore, it is necessary to investigate what happens when particulate matter serves as substrate since previous results have indicated that GO wraps starch granules and therefore prevents its hydrolysis. In fact, the envelope of starch granules is given by the interaction of the oxygenated groups of GO, which have negative charge, and the hydroxyl groups in starch, which have positive charge.¹⁷ The above opens the questions on what interactions between rGO and starch occur and what will be the effects when all these components are present in anaerobic digestion processes.

Starch is an energy reserve in plants and the second most abundant biopolymer on Earth. It is mainly composed of two types of polysaccharides, amylose and amylopectin, which are organized in multilevel structures of increasing complexity. Starch granules are structures that vary in size (1-200 μm) and shape (ovals, spheres, polygons, etc.) depending on the botanical origin. Starch is of great importance within the food industry and is taking relevance every day in other industrial areas, such as the manufacture of biodegradable materials.¹⁸⁻²¹ Glucose, on the other hand, can be released from starch hydrolysis and is a common constituent of different industrial wastewaters.

The aim of the present work was to study the acute effects of rGO on the methanogenic activity of an anaerobic consortium supplied with two different substrates: glucose as a soluble model substrate and starch as a particulate model substrate. The goal of the study is to provide evidence to understand the interactions of rGO, with different reduction degrees, within the methanogenic consortium.

Materials and methods

Materials and chemical reagents

GO was purchased from Graphene Supermarket® and has the following characteristics: concentration 6.2 g/L in aqueous dispersion, monolayer >80%, nominal particle size between 0.5 and 5 μm , C/O ratio 3.95. Ascorbic acid (L-AA, ACS grade) was obtained from Golden

Bell® (Mexico City, Mexico), while starch, glucose and all other reagents used in this work were reactive grade from either Sigma-Aldrich Company or Merck.

Solutions

The basal medium used for sludge activation was composed of (mg/L): NH_4Cl (280), K_2HPO_4 (250), $\text{MgSO}_4 \cdot 7\text{H}_2\text{O}$ (100), $\text{CaCl}_2 \cdot 2\text{H}_2\text{O}$ (10), NaHCO_3 (5000) and 1 mL/L of trace elements solution composed of (mg/L): $\text{FeCl}_2 \cdot 4\text{H}_2\text{O}$ (2000), H_3BO_3 (50), ZnCl_2 (50), $\text{CuCl}_2 \cdot 2\text{H}_2\text{O}$ (38), $\text{MnCl}_2 \cdot 4\text{H}_2\text{O}$ (500), $(\text{NH}_4)_6\text{Mo}_7\text{O}_{24} \cdot 4\text{H}_2\text{O}$ (50), $\text{AlCl}_3 \cdot 6\text{H}_2\text{O}$ (90), $\text{CoCl}_2 \cdot 6\text{H}_2\text{O}$ (2000), $\text{NiCl}_2 \cdot 6\text{H}_2\text{O}$ (92), $\text{Na}_2\text{SeO}_3 \cdot 6\text{H}_2\text{O}$ (162), EDTA (1000) and 1 mL HCl (36%); pH was adjusted to 7.0 ± 0.2 using NaOH or HCl 0.1 N. In the case of batch assays, NaHCO_3 was adjusted to 3.13 g/L in order to obtain a pH of 7 in combination with a mixture of N_2/CO_2 (80%/20%, v/v) used as headspace. Distilled water was used to prepare all solutions.

Chemical reduction of GO

Reduction of GO was carried out according to Toral-Sánchez et al.¹⁵ Briefly, 10 mL of GO solutions (0.1 mg/mL) and 100 mg of ascorbic acid were placed in a 30 mL beaker. Immediately, samples were vigorously stirred at room temperature. In order to obtain materials with different reduction degrees, reduction kinetics were carried out for 1, 2 and 4 h. After the reduction time, samples were centrifuged at 10,000 rpm for 20 min in order to remove all ascorbic acid remaining by decantation. Recovered rGO was rinsed with deionized water three times, then dispersed in deionized water, and finally sonicated for 30

min. rGO materials obtained from 1, 2 and 4 hours of reduction are referred to as rGO1, rGO2 and rGO4, respectively, in the present study.

The concentration of the three rGO dispersions was measured by a gravimetric method, which implied drying 1 mL of the dispersions in vials at constant weight at 45 °C under vacuum and 1400 rpm for 6 hours using Vacufuge plus Eppendorf concentrator equipment.

Characterization of materials

Spectroscopic characterization

Functional groups of rGO1, rGO2 and rGO4 were identified by Fourier transform infrared spectroscopy (FTIR) using a Thermo-Nicolet 6700 FT-IR equipment. Samples were prepared using materials, which were dried for 4 h into a Vacufuge plus Eppendorf concentrator equipment at 45 °C under vacuum and 1400 rpm, mixed with KBr in a 1:1000 ratio, respectively, and compressed to form pellets. The pellets were analyzed by transmission under conditions of 128 scans, resolution of 4 cm⁻¹, CO₂ and H₂O automatic correction.

The reduction degree of the materials, rGO1, rGO2 and rGO4, was also studied by Raman spectroscopy using a RENISHAW Micro-Raman Invia spectrometer with laser frequency of 532 nm as excitation source through a 50× objective. The sample preparation implied the formation of films on aluminum foil by dripping deposition of each material dispersions, and then allowed to dry for 12 h prior to analysis.

Particle charge and size distribution

Zeta potential (ζ) measurements were performed in aqueous solution for rGO1, rGO2 and rGO4 at pH of 7, which is the pH value of the biological experiments performed. For this purpose, dispersions of 150 mg/L of each rGO material were adjusted to the desired pH value using NaOH or HCl 0.1 N as needed until the variation of pH values was less than 0.5 in measurements conducted every 5 h. After pH stabilization, 1 mL of the sample was sonicated using a Bransonic model B2510-DTH equipment at 40 kHz for 10 s and immediately placed into the MICROTRAC Zetatrac NPA152-31A cell. Size distribution was measured by Dynamic Light Scattering, using the same equipment, at pH 7 and with the same sample preparation mentioned before.

Scanning electron microscopy (SEM)

Micrographs of rGO materials and starch were obtained with a FEI Helios Nanolab 600 Dual Beam Scanning Electron Microscope, operated at 5.00 kV and 86 pA, and elemental analyses were carried out by energy dispersive spectrometer (EDS) with the same equipment. Samples were prepared on silicon wafers by dripping deposition and were dried under ambient conditions overnight before microscope observation. Biological samples were examined using a FEI model Quanta 250 SEM, adjusted to 25 kV, spot size 4.5 and WD 10 mm, recording the micrographs using an Everhart Thornley Detector.

Biological assays

Inoculum

Methanogenic granular sludge was obtained from a full-scale up-flow anaerobic sludge bed reactor treating brewery wastewater (Mahou, Guadalajara, Spain). The sludge was stored at 4 °C and it was washed and crushed using a needle gauge 22G before its use in the incubations. The content of volatile solids (VS) of the sludge was 6.96% of wet weight.

Sludge incubations with rGO

Batch assays were conducted in triplicates using serological bottles of 60 mL of volume. In these experiments, 9 mL of basal medium containing starch or glucose (final concentration of 2 g chemical oxygen demand (COD)/L) and 1.5 g VS/L of sludge were added to each bottle and then flushed with a gas mixture of N₂/CO₂ (80:20, v/v) for 3 min. Subsequently, bottles were sealed, and the headspace was further flushed using the same gas mixture for 3 min. The bottles were incubated overnight at 30 °C in an orbital shaker at 120 rpm for biomass activation. After this period, 1 mL of deionized water was added to the control bottles and 1 mL from the corresponding stock solution of rGO material to amended cultures (10 mL as total volume in all cases) in order to get a concentration of 300 mg/L of each GO material. Once the GO materials were added, the headspace of all bottles was flushed again with the N₂/CO₂ gas mixture for 3 min and incubated at 30 °C in an orbital shaker at 120 rpm. Gas samples (100 µL) were periodically taken for methane measurement by gas chromatography as previously described.⁸ Methane concentration was plotted against time to obtain the maximum slope by linear regression from at least three points throughout the incubation period and the maximum methanogenic activity (MMA) was then calculated.

Results and discussion

Physical characterization of rGO

As known, zeta potential provides the materials surface charge. The results of the present study revealed zeta potential values of -16.5 mV, 0.284 mV, 0.565 mV and 4.453 mV for GO, rGO1, rGO2, rGO4, respectively, at pH 7. These data indicate that the higher the reduction time to produce the rGO samples, the higher the zeta potential value obtained, which is related to the loss of oxygenated functional groups through the reduction process. In other words, the lower the concentration of oxygen-containing groups in GO materials, the more positive the materials surface charge. These results agreed with FTIR analysis, which revealed the loss of some oxygenated functional groups through the reduction process and indicated the prevalence of hydroxyl groups, which possess partial positive charge at pH 7.

The reduction process turned GO sheets more hydrophobic, so that they tended to stack among them due to π interactions of the aromatic rings. Consequently, size distribution moved to larger size of particles consistent with the increase in reduction time. Besides, low values in ζ mean instability of colloidal dispersion, thus rGO sheets agglomerate easily. Taking all these aspects into account, Fig.1 makes sense since most rGO1 particles showed a size of 687 nm, while rGO2 particles were divided between sizes of 687 nm (37.4%) and 818 nm (34.7%). Finally, rGO4 particles predominated with a size of 818 nm.

The morphology of GO and rGO materials was studied by SEM. Obtained images revealed that GO is thinner, shows cracks and tends to fold over itself, while rGO materials have thicker lamellae, due to the stacking of rGO sheets caused by the reduction treatment. Furthermore, the extended sections found in the samples presented changes in transparency and the way they fold; for example, lamellae of rGO2 and rGO4 were smoother and apparently more rigid/denser, while rGO1 still presented fine sheets (see Fig. 2).

In the case of graphene materials mixed with starch, SEM images (Fig. 3) show that GO perfectly wraps starch granules (Fig.3b), even following the shape of those that were broken by the preparation procedure. Granules were easily found in examined samples, but when the mixture contained any of the rGO materials, much smaller clusters were observed (rGO4 in Fig. 3c). These clusters are essentially crystals from the basal medium, rGO sheets, and particles with spherical/polyhedral and rod-like shapes (Fig.3d). The observed clusters agree with the hierarchical structures integrating starch granules, being consistent with blocklets and super helical structures, which seemed to be composed of a mixture of A-type and B-type crystalline polymorphs that give them that “Cheetos-type” shape.^{21, 22} These findings indicate that rGO materials did not cover starch granules but broke them into smaller sub-structures. The latter suggests that rGO materials promoted the disintegration of starch granules, possibly due to catalytic activity of remaining carboxylic groups and/or defects at edges of rGO sheets with unpaired electrons.^{23, 24} However, further research is needed to clarify what are the mechanisms that give rise to the observed results.

When collected samples were observed, it was possible to find starch granules attached to exopolysaccharides, bacteria and rGO sheets. Nevertheless, rGO sheets never wrapped starch granules (rGO4 in Fig. 3e) as previously reported with GO,¹⁷ so that they were always interacting with cells and exopolysaccharides (Fig. 3f). These results show that rGO preferentially adheres to bacteria, which have a negative surface charge,²⁵ while as it was shown by the results of ζ values, rGO had a greater positive charge by increasing the reduction time. Nonetheless, it must be considered that bacteria can adhere to rGO sheets, because they serve as conductive material favoring DIET and facilitating bacterial growth.²⁶

Spectroscopic characterization of GO and rGO

Raman spectra (Fig. 4) of synthesized rGO materials and the original GO displayed the characteristic D and G bands of carbon at $\sim 1350\text{ cm}^{-1}$ and $\sim 1600\text{ cm}^{-1}$, respectively. D band is associated with disorder-induced symmetry-breaking effects of sp^2 network, while G band is related with the ordered structure of graphene hexagons and graphite crystallinity. Additionally, Raman spectra show the 2D band at $\sim 2676\text{ cm}^{-1}$, which is sensitive to the π bond in the graphitic electronic structure and the number of layer. Also, D+G band at $\sim 2950\text{ cm}^{-1}$ is observed, which is the combination of bands D and G induced by disorder.²⁷

The ratio I_D/I_G provides information of the amount of disorder linked to an oxidation process, but in the case of a reduction process, the I_D/I_G ratio has been reported to rise by increasing the reduction degree of GO. This could be corroborated by the I_D/I_G ratios obtained for GO, rGO1, rGO2 and rGO4, which were 0.809, 1.011, 1.124 and 1.011, respectively. The

previous values show small difference among the reduced materials; thus, the I_{2D}/I_G ratio was calculated since it has relationship with the measurement of sp^2 regions and with electron mobility.²⁸ The values of the I_{2D}/I_G ratio for GO, rGO1, rGO2 and rGO4 were 0.164, 0.386, 0.295 and 0.278, respectively, and indicate larger graphitic domains and consequently higher electron mobility in the reduced materials. Nevertheless, the observed trend for I_D/I_G and I_{2D}/I_G ratios disagrees with the expected increase in graphitization with increased reduction time. The observed trend seems to point out that the reduction process is also creating defects, something that is commonly seen in thermal reduction.²⁹ Additionally, the shape of the 2D band indicates the presence of multilayer rGO,²³ which agrees with observations collected by SEM images.

FTIR spectra in Fig. 5 show the presence of oxygenated functional groups in GO at 3300 cm^{-1} , 1730 cm^{-1} , 1200 cm^{-1} and 1100 cm^{-1} associated with $-\text{OH}$, $-\text{C}=\text{O}$, $-\text{C}-\text{O}-\text{C}$ and $-\text{C}-\text{O}$, respectively. The reduction time triggered a decrease on the intensity of the bands related with $-\text{C}=\text{O}$, $-\text{C}-\text{O}-\text{C}$ and $-\text{C}-\text{O}$, suggesting that these groups were partly reduced in GO by the reducing process with ascorbic acid. The intensity of those groups decreased in agreement with longer reducing time, being rGO4 the material with the lowest content of these functional groups. In contrast, the $\text{C}=\text{C}$ band prevailed independently of the reduction time since these groups did not react with ascorbic acid. Interestingly, only the spectrum corresponding to rGO1 displayed a band at 2900 cm^{-1} , which is attributed to $\text{C}-\text{H}$ groups together with a drastic decrease in the intensity of the band associated with the epoxy groups.

However, the band of –OH showed a narrowing, while its intensity seemed to be the same. This phenomenon could be explained considering that hydrophobicity increased with the reduction degree of GO sheets, so that the amount of water physisorbed or intercalated among stacks of rGO sheets would be less.³⁰ Moreover, the prevalence of the band related to –OH groups agree with reports about the stability of these groups as compared to epoxy groups (–C–O–C) under the conditions prevailing in the reduction process. FTIR spectra also agree with information indicating that epoxy groups are the most abundant and the most reactive,² since they displayed a band with high intensity in the GO spectrum and the intensity decreased with the increase of reduction time.

Acute effects of rGO materials on methanogenesis

Sludge exposed to rGO with different extent of reduction revealed a positive effect on methanogenesis with both glucose (Fig. 6a) and starch (Fig. 6c) as substrates. This positive effect improved the amount of methane produced as well as the MMA. The most relevant increase occurred in sludge incubations performed with starch, in which the difference between the treatments with rGO and the control incubated without rGO is highly evident. MMA could be calculated from the kinetic data (Table 1). For experiments performed with glucose, it was observed that rGO1 increased 4.7% the MMA, while rGO2 and rGO4 promoted an enhancement of 13.8% and 8.9%, respectively, with respect to the control incubated in the absence of rGO materials (Fig. 6b). Furthermore, rGO materials greatly enhanced methane production in sludge incubations conducted with starch, especially with

rGO1, which triggered an improvement of 114% on the MMA as compared to the control treatment prepared without rGO materials. Meanwhile, materials rGO4 and rGO2 increased the MMA by 86.4% and 70.6%, respectively, with respect to the control when starch was provided as electron donor (Fig. 6d). These results suggest that rGO materials did not cover starch granules, which was shown to occur in sludge incubations conducted with GO.¹⁷ Wrapping of starch granules by GO sheets caused mass transfer limitations negatively affecting the methanogenic activity of anaerobic sludge.¹⁷

In experiments performed with starch, it was observed that the highest methane production was obtained with rGO1, which makes sense when considering the smaller particle size of this conductive material as compared to the other reduced materials. Namely, rGO1 has a greater exposed surface area than rGO2 and rGO4 and therefore greater interaction with starch granules. However, contrary to what was observed in experiments conducted with GO,¹³ the interactions with rGO1 promoted the disintegration of starch granules. This may be due to the removal of epoxy groups through the reducing process of GO to rGO since these functional groups were responsible for the wrapping of starch granules by GO.¹⁷ Moreover, carbonyl functional groups, which prevail mainly at the edges of graphene sheets³¹ can interact with the hydroxyl groups of the polysaccharide chains by hydrogen bonding, thus fragmenting starch granules and producing the structures observed in Fig. 3d. In addition to the disintegration of the starch granules, according to collected Raman spectra, rGO1 also showed a great mobility of electrons, which can favor DIET. On the other hand, the lower

MMA observed in sludge incubations amended with rGO2 or rGO4 as compared to those performed with rGO1 could be due to agglomeration of rGO sheets in rGO2 and rGO4, with the resulting decrease in surface area. Additionally, a decrease in carbonyl groups in rGO2 and rGO4 (Fig. 5) could also explain the worse catalytic effect stimulated by these materials on methane production.

The positive effects of rGO on anaerobic digestion reported here could be explained by different aspects. In the case of micro-structures, they provide available surface and porosity, which may protect microorganisms by creating a micro-environment. Additionally, functional groups on the materials surface could serve as electron shuttles and their conductivity could be involved in DIET. Moreover, large surface area promotes adsorption of substrates, which are easily accessible to microorganisms attached to the materials. Furthermore, rGO could also play a buffering role against abrupt changes in concentration of inhibitors and it promotes disintegration of particulate organic matter improving the hydrolysis stage. The electrostatic interactions among microorganisms and their exopolymeric substances with rGO sheets and starch granules, discussed above and shown in Figure 3, may also explain the greater enhancement observed in the MMA through incubations performed with starch as compared to those conducted with glucose. Furthermore, while addition of rGO consistently improved the MMA observed in the studied consortium, there was not a clear trend depending on the extent of reduction of GO. Thus, further studies are required to elucidate the interactions prevailing among bacteria, rGO

Accepted Article

sheets and substrate particles, which ultimately may govern the methanogenic activities in anaerobic consortia.

Conclusions

The effects of GO with different degree of reduction were studied and the results indicate that rGO promotes the methanogenic activity of an anaerobic consortium provided with a soluble (glucose) or a particulate (starch) substrate. Interactions of rGO with starch granules appeared especially important depending on the degree of reduction of GO, which directly affects the disintegration of starch granules. Oxygenated groups present in the surface of rGO interacted with the hydroxyl groups of starch polysaccharides promoting disintegration of the granules into smaller elements, which increases the specific area and thus enhanced the hydrolysis step. The knowledge generated by this study allows to predict the effects of the different materials derived from GO when applied to anaerobic digestion processes.

Acknowledgements

The program Frontiers in Science of CONACYT (Project 1289) and Universidad Nacional Autónoma de México (UNAM, project 9407 and Grant PAPIIT No. TA100120) financially supported this work. J.I. Bueno-López thanks for the scholarship received from Tecnológico Nacional de México. Additionally, the authors acknowledge the technical support provided by D. Partida-Gutiérrez, J.P. Rodas-Ortiz, M. Delgado-Cardoso, E. Vences-Alvarez, A.

Patrón-Soberano, A.I. Peña-Maldonado, B. Rivera-Escoto and R. Santoyo-Cisneros. We also greatly acknowledge the use of infrastructure from the National Laboratory, LINAN-IPICYT.

References

1. Rogala M, Dabrowski P, Kowalczyk PJ, Wlasny I, Kozlowski W, Busiakiewicz A, Karaduman I, Lipinska L, Baranowski JM, Klusek Z, The observer effect in graphene oxide – How the standard measurements affect the chemical and electronic structure. *Carbon* **103**:235–241 (2016).
2. Dreyer DR, Park S, Bielawski CW, Ruoff RS, The chemistry of graphene oxide. *Chem Soc Rev* **39**:228–240 (2010).
3. De Silva KKH, Huang H-H, Joshi RK, Yoshimura M, Chemical reduction of graphene oxide using green reductants. *Carbon* **119**:190–199 (2017).
4. Yaragalla S, Rajendran R, Jose J, Almaadeed MA, Kalarikkal N, Thomas S, Preparation and characterization of green graphene using grape seed extract for bioapplications. *Mat Sci Eng C* **65**:345-353 (2016).
5. Yaragalla S, Rajendran R, Almaadeed MA, Kalarikkal N, Thomas S, Chemical modification of graphene with grape seed extract: Its structural, optical and antimicrobial properties. *Mat Sci Eng C* **102**:305-314 (2019).

6. Karmakar A, Mallick T, Das S, Begum NA, Naturally occurring green multifunctional agents: Exploration of their roles in the world of graphene and related systems. *Nanostructures & Nano-Objects* **13**: 1-20 (2018).
7. Salas EC, Sun Z, Lüttge A, Tour JM, Reduction of Graphene Oxide via Bacterial Respiration. *ACS Nano* **4**:4852–4856 (2010).
8. Wang G, Qian F, Saltikov CW, Jiao Y, Li Y, Microbial reduction of graphene oxide by *Shewanella*. *Nano Res* **4**:563–570 (2011).
9. De Velasco-Maldonado PS, Pat-Espadas AM, Cházaro-Ruíz LF, Cervantes FJ, Hernández-Montoya V, Cold oxygen plasma induces changes on the Surface of carbon materials enhancing methanogenesis and N₂O reduction in anaerobic sludge incubations. *J Chem Technol Biotechnol* **94**:3367-3374 (2019).
10. Xu S, He C, Luo L, Lü F, He P, Cui L, Comparing activated carbon of different particle sizes on enhancing methane generation in upflow anaerobic digester. *Bioresour Technol* **196**:606–612 (2015).
11. Amezquita-Garcia HJ, Rangel-Mendez JR, Cervantes FJ, Razo-Flores E, Activated carbon fibers with redox-active functionalities improves the continuous anaerobic biotransformation of 4-nitrophenol. *Chem Eng J* **286**:208–215 (2016).

12. Colunga A, Rangel-Mendez JR, Celis LB, Cervantes FJ, Graphene oxide as electron shuttle for increased redox conversion of contaminants under methanogenic and sulfate-reducing conditions. *Bioresour Technol* **175**:309–314 (2015).
13. Salvador AF, Martins G, Melle-Franco M, Serpa R, Stams AJM, Cavaleiro AJ, Pereira MA, Alves MM, Carbon nanotubes accelerate methane production in pure cultures of methanogens and in a syntrophic coculture. *Environ Microbiol* **19**:2727–2739 (2017).
14. Tian T, Qiao S, Li X, Zhang M, Zhou J, Nano-graphene induced positive effects on methanogenesis in anaerobic digestion. *Bioresour Technol* **224**:41-47 (2017).
15. Toral-Sánchez E, Ascacio Valdés JA, Aguilar CN, Cervantes FJ, Rangel-Mendez JR, Role of the intrinsic properties of partially reduced graphene oxides on the chemical transformation of iopromide. *Carbon* **99**:456–465 (2016).
16. Toral-Sánchez E, Rangel-Mendez JR, Ascacio Valdés JA, Aguilar CN, Cervantes FJ, Tailoring partially reduced graphene oxide as redox mediator for enhanced biotransformation of iopromide under methanogenic and sulfate-reducing conditions. *Bioresour Technol* **223**:269–276 (2017).
17. Bueno-López JI, Rangel-Mendez JR, Alatríste-Mondragón F, Pérez-Rodríguez F, Hernández-Montoya V, Cervantes FJ, Graphene oxide triggers mass transfer limitations

on the methanogenic activity of an anaerobic consortium with a particulate substrate. *Chemosphere* **211**:709–716 (2018).

18. Xie F, Pollet E, Halley PJ, Avrous L, Starch-based nano-biocomposites. *Prog Polym Sci* **38**:1590–1628 (2013).
19. Hoover R, Composition, molecular structure, and physicochemical properties of tuber and root starches: A review. *Carbohydr Polym* **45**:253–267 (2001).
20. Vanier NL, El Halal SLM, Dias ARG, da Rosa Zavareze E, Molecular structure, functionality and applications of oxidized starches: A review. *Food Chem* **221**:1546–1559 (2017).
21. Pérez S, Bertoft E, The molecular structures of starch components and their contribution to the architecture of starch granules: A comprehensive review. *Starch/Staerke*. WILEY-VCH Verlag (2010).
22. Bras J, Dufresne A, Starch Nanoparticles: A Review. *Biomacromolecules* **11**:1139–1153 (2010).
23. Su C, Acik M, Takai K, Lu J, Hao S, Zheng Y, Wu P, Bao Q, Enoki T, Chabal YJ, Ping Loh K, Probing the catalytic activity of porous graphene oxide and the origin of this behaviour. *Nat Commun* **3**:1298 (2012).

24. Song Y, Qu K, Zhao C, Ren J, Qu X, Graphene oxide: Intrinsic peroxidase catalytic activity and its application to glucose detection. *Adv Mater* **22**:2206–2210 (2010).
25. Alvarez LH, Cervantes FJ, Assessing the impact of alumina nanoparticles in an anaerobic consortium: methanogenic and humus reducing activity. *Appl. Microbiol. Biotechnol.* **95**:1323-1331 (2012).
26. Rotaru A-E, Calabrese F, Stryhanyuk H, Musat F, Shrestha PM, Weber HS, Snoeyenbos-West OLO, Hall POJ, Richnow HH, Musat N, Thamdrup B, Conductive particles enable syntrophic acetate oxidation between *Geobacter* and *Methanosarcina* from coastal sediments. *mBio* **9**:e00226-18 (2018).
27. Ferrari AC, Raman spectroscopy of graphene and graphite: Disorder, electron–phonon coupling, doping and nonadiabatic effects. *Solid State Commun* **143**:47–57 (2007).
28. Raza, H. (Ed.), Graphene Nanoelectronics. NanoScience and Technology. *Springer* Berlin, Heidelberg (2012).
29. Lin L-C, Grossman JC, Atomistic understandings of reduced graphene oxide as an ultrathin-film nanoporous membrane for separations. *Nat Commun* **6** (2015).
30. Acik M, Lee G, Mattevi C, Pirkle A, Wallace RM, Chhowalla M, Cho K, Chabal Y, The Role of Oxygen during Thermal Reduction of Graphene Oxide Studied by Infrared Absorption Spectroscopy. *J Phys Chem C* **115**:19761–19781 (2011).

31. Pei S, Cheng H-M, The reduction of graphene oxide. *Carbon* **50**:3210–3228 (2012).

Figures Captions

Fig. 1. Size distribution of GO and rGO materials. Bars represent the percentage of particles of a given size, while curves were added to show the pattern of size distribution due to the reduction process.

Fig. 2. SEM images of untreated GO and reduced materials obtained at increasing reduction time (rGO1, rGO2 and rGO4).

Fig. 3. SEM images of pristine starch granules (a), mixture of starch and GO (b), clusters found in samples with rGO4 (c), structures inside the clusters (d) and a sample of the bioassays using starch and rGO4 at low (e) and high magnification (f).

Fig. 4. Raman spectra of reduced and unreduced GO materials showing the main bands of carbonaceous materials.

Fig. 5. FTIR spectra of reduced and unreduced materials. Shaded areas indicate the regions of the oxygenated functional groups that underwent changes throughout the reduction process.

Fig. 6. Cumulative methane obtained with glucose (a) and starch (c) and their corresponding maximum methanogenic activity (MMA; b and d) Numbers displayed in the series legend indicate the concentration (mg/L) of rGO1, rGO2 and rGO4. Letters on top of bars show statistical difference ($p < 0.05$) respect to the control incubated in the absence of rGO materials (letter a) and between treatments (letter b). Same set of letters means no statistically difference.

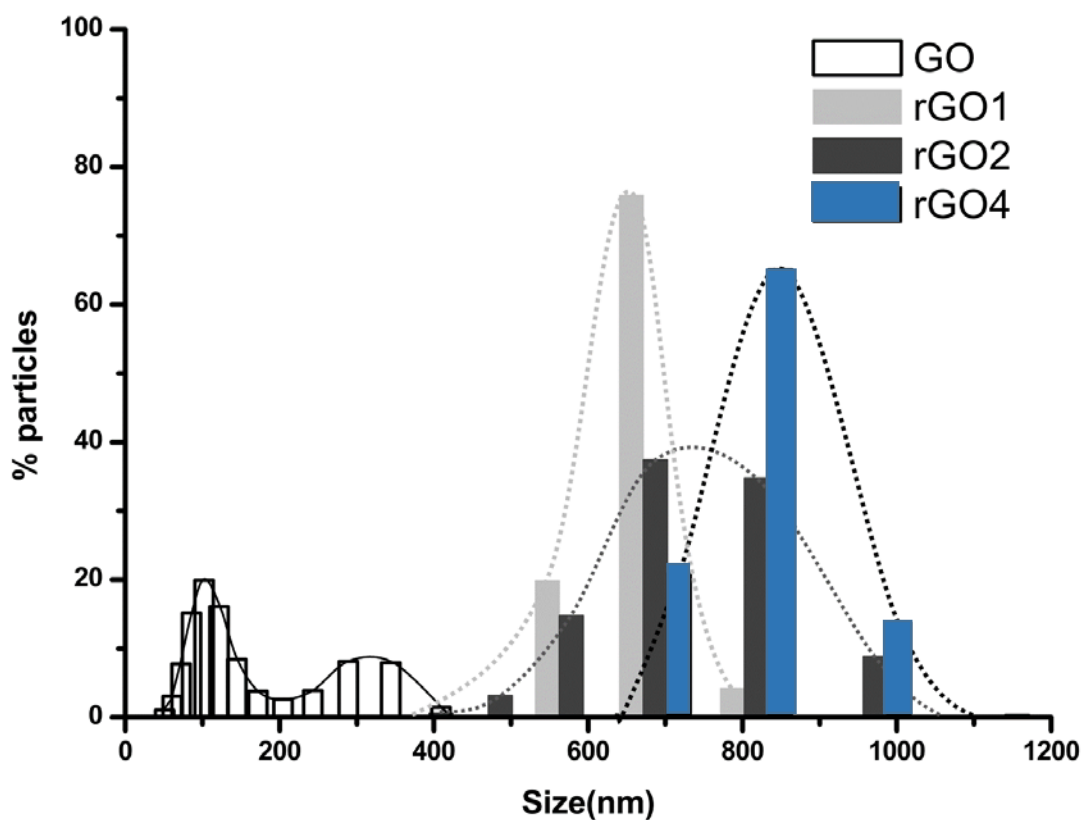


Fig. 1.

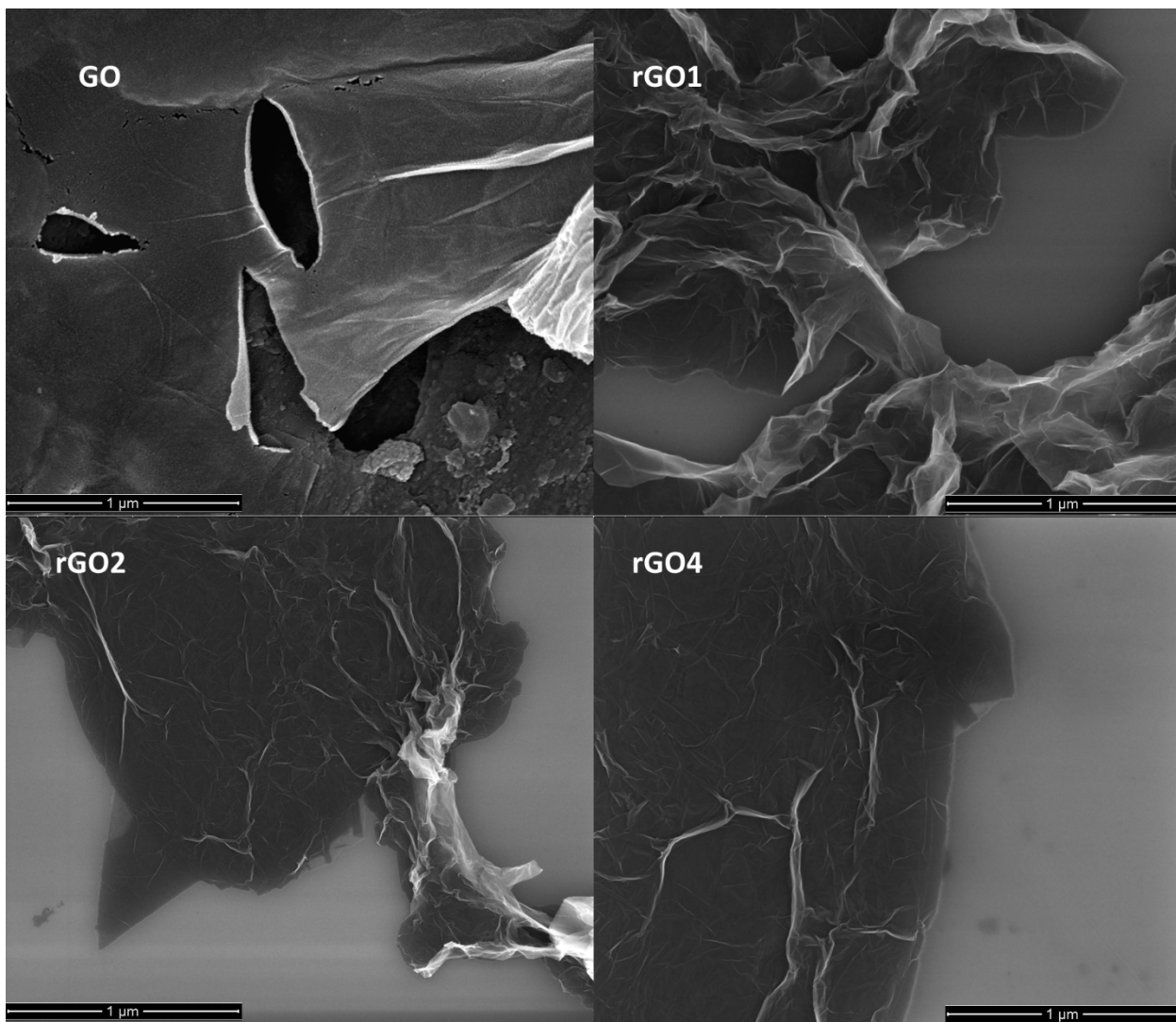


Fig. 2.

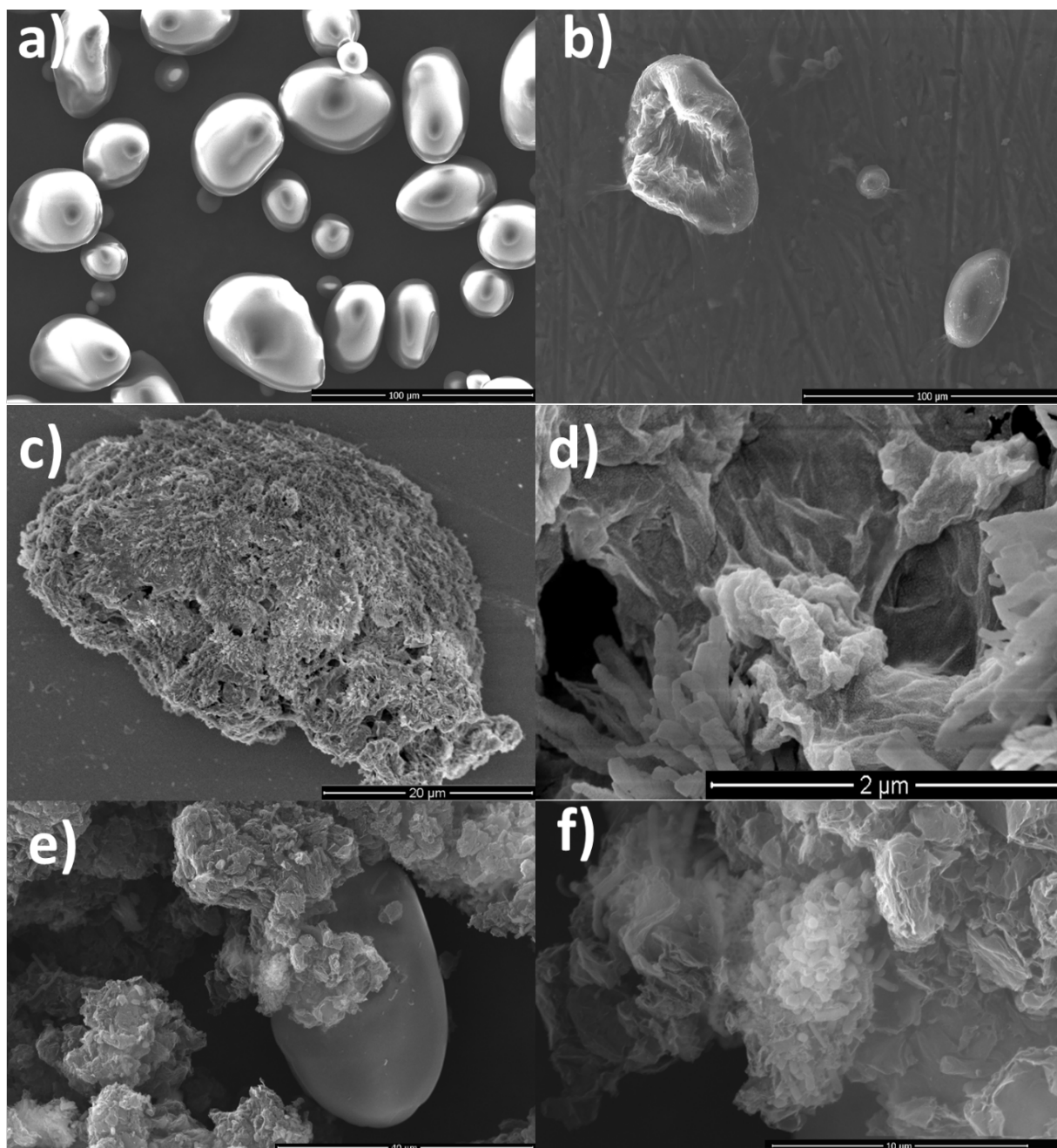


Fig. 3.

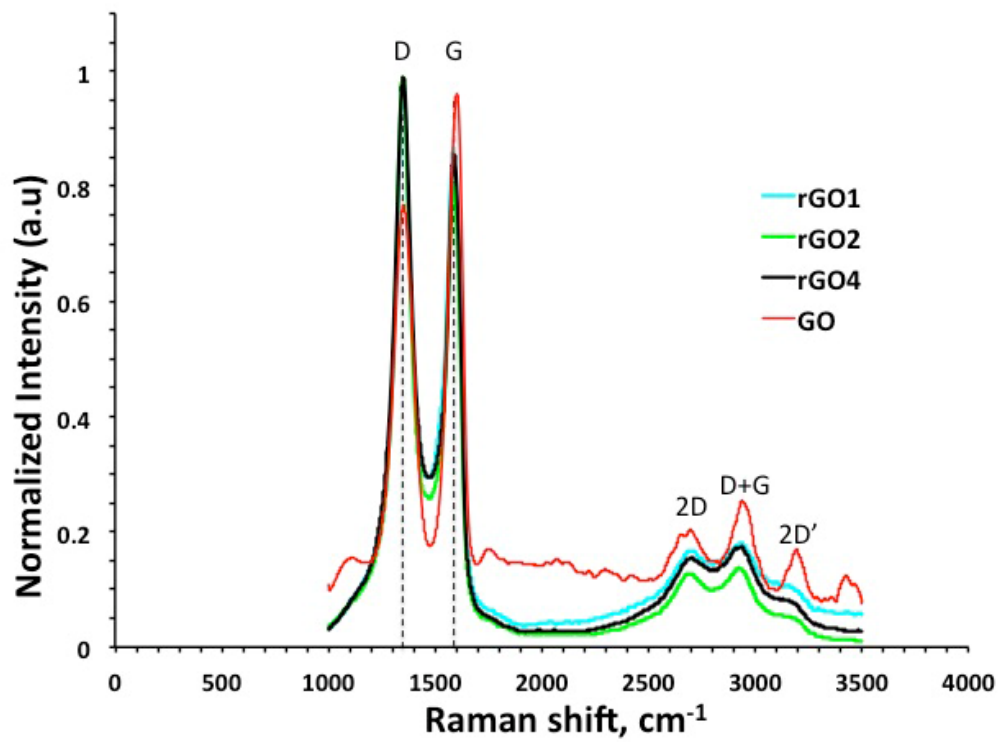


Fig. 4.

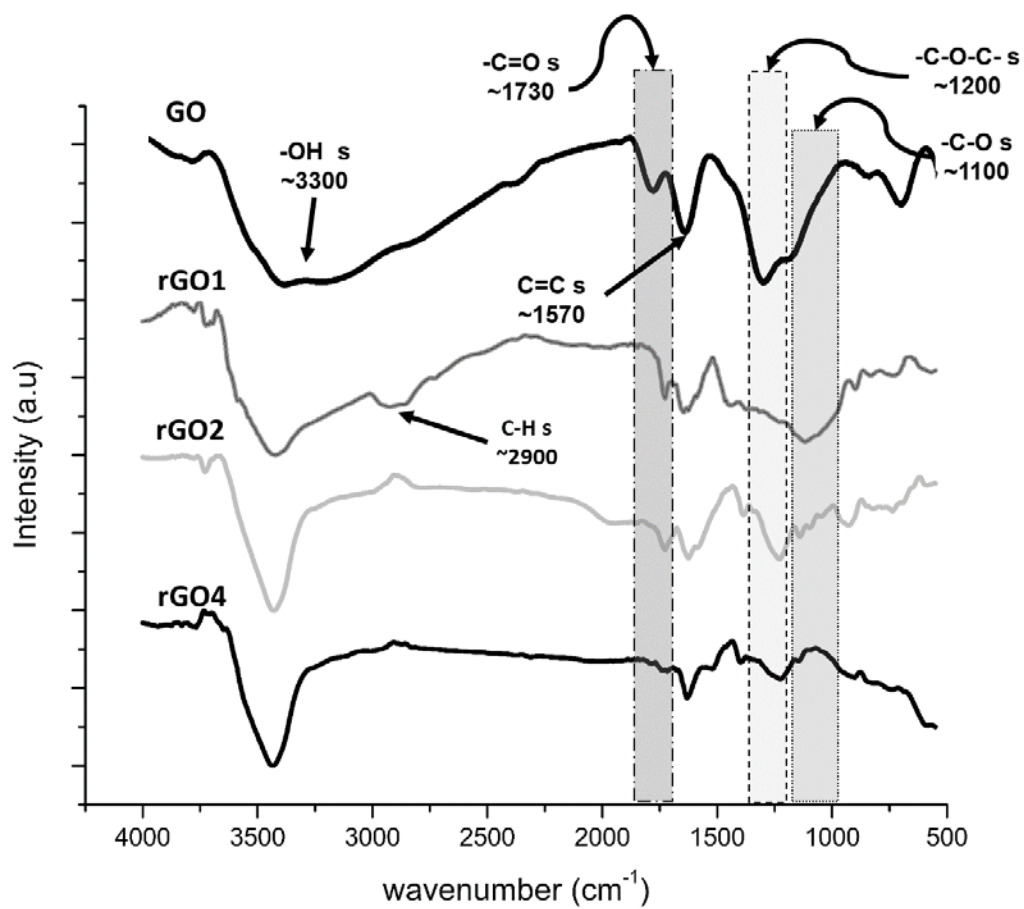


Fig. 5.

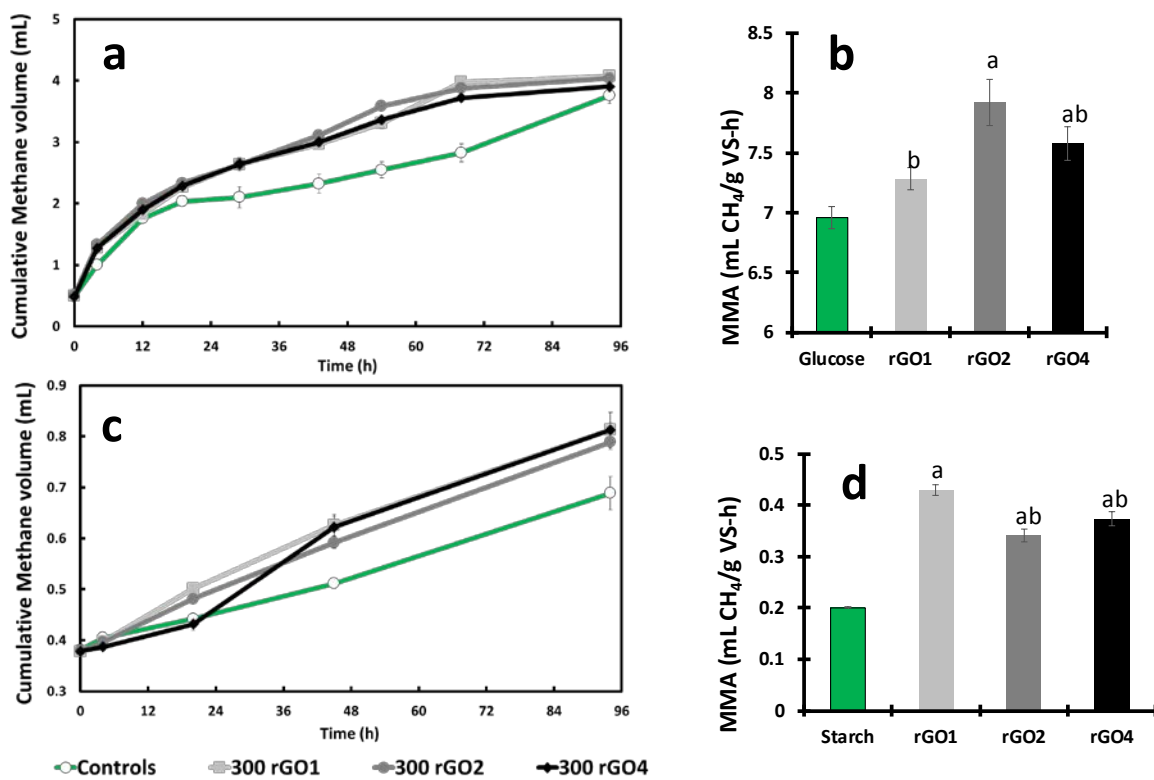


Fig. 6.

Table 1. Maximum methanogenic activity (MMA) obtained for experiments performed with glucose or starch and rGO with different reduction degrees

Treatment	Glucose		Starch	
	MMA ^a ± SD	Treatment effect ^b (%)	MMA ^a ± SD	Treatment effect ^b (%)
Control without rGO	7.0 ± 0.1	-	0.20 ± 0.01	-
rGO1	7.3 ± 0.1	4.7	0.43 ± 0.01	114.1
rGO2	7.9 ± 0.2	13.8	0.34 ± 0.01	70.6
rGO4	7.6 ± 0.1	8.9	0.37 ± 0.01	86.4

^aMaximum methanogenic activity calculated from 3 points of the kinetic data by linear regression (mL CH₄ /g VS-h). ^bTreatment effects are the difference on MMA using rGO (300 mg/L) compared to control treatments without rGO.